Design and Testing of an Olfactory Stimulus Presentation Device for use in Functional Magnetic Resonance Imaging (fMRI)

by

Shawn Keating 0671512

Electrical and Biomedical Engineering

Faculty Supervisors: Dr. Aleksandar Jeremic, Dr. Michael Noseworthy

McMaster University

Hamilton, Ontario Canada

April 9th, 2010

Copyright © April 2010 by Shawn Keating

ABSTRACT

Olfaction is an ancient and complex chemosensory process that for many animals serves as their main sensory link with the surrounding environment. In the field of functional brain imaging, it is a process that has been largely unstudied due to many complicating factors such as the qualitative nature of olfaction, the difficulty of providing stimuli in a controlled manner, and the non-superficial location of the main olfactory centers of the brain. The goal of this project was to develop an MRI compatible device for generation and presentation of olfactory stimulus for use in functional imaging of the olfactory response. After taking into consideration various constraints in the design process, the final device design consists of a scented liquid that is nebulised in an Erlenmeyer flask by pressurized medical air and subsequently transported through chemically inert tubing to a modified ventilator mask secured to the subject. To test the device, functional magnetic resonance imaging (fMRI) analysis was performed with an experimental protocol that provided stimulus for a period of 30 seconds and allowed it to clear for 90 seconds. This procedure was repeated over 5 cycles starting with 90 seconds of no stimulus resulting in a total time of 10 minutes. Statistical analysis was performed on the resulting images from two of the three fMRI experiments undertaken and the results of the last trial show activation of deep areas of the brain commonly associated with olfaction and described in existing publications on the topic. This is a promising result given the number of trials undertaken and the simplistic nature of the overall experimental protocol. Therefore, the conclusion is that with increased time and funding the basic device and experimental protocols presented in this project could easily be expanded to assist in a functional characterization of the olfactory response.

Keywords: olfaction, odorant, functional magnetic resonance imaging, brain imaging.

ACKNOWLEDGEMENTS

Many thanks to Dr. Michael Noseworthy for donating his time and MRI suite to allow this project to take shape. His expertise on statistical analysis of fMRI image sets was also invaluable.

Thanks also to Dr. Aleksandar Jeremic for suggesting the topic of the project and for his assistance in the experimental procedure.

TABLE OF CONTENTS

LIST OF FIGURES

NOMENCLATURE

Diamagnetic- a material whose paired electrons induce a magnetic field in the opposite direction of the applied external magnetic field resulting in a weak repulsive effect.

Haemoglobin- complex molecule found in red blood cells used for the transfer of oxygen and carbon dioxide between the blood and tissue.

Nebulizer- a device that induces a liquid to form an aerosol by exposing it to compressed air inside a closed container.

Olfaction- concerns the binding of an odorant to its receptor in the nose through to the generation of a neurological response (the sense of smell).

Paramagnetic- a material with unpaired electrons that has an induced magnetism in the presence of an external magnetic field.

Vapour Pressure- an inherent property of a liquid that determines the external pressure at which it spontaneously converts from liquid to gaseous state.

Voxel- a volume element in an image data set.

1. INTRODUCTION

Olfaction is an ancient and complex chemosensory process that for many animals represents their closest contact to the physical world. Even in the relatively underdeveloped human system it requires an incredible 1.5% of the entire genome for normal operation. [1] Exposure to an odorant in the environment leads to the activation of numerous emotionally charged pathways in the brain. If these pathways could be stimulated in an experimentally controlled manner, the olfactory system has the potential to become a powerful tool for studying functional activation in the deep centers of the brain.

1.1. Background

1.1.1. Olfaction

Over 1000 distinct odorant molecules can be distinguished by chemoreceptors on the olfactory epithelium at the back of the nose. [2] Each epithelial cell expresses only one type of chemoreceptor and converts the chemical binding of its odorant to an action potential that travels down its axon and into the olfactory bulb (Figure 1.1). [3] Axons of the mitral and tuft cells in the olfactory bulb project into an area collectively known as the primary olfactory cortex. This area includes the anterior olfactory nucleus, olfactory tubercle and the piriform cortex. Projections out of the piriform cortex synapse with secondary olfactory areas, most notably the amygdala, entorhinal cortex, orbitofrontal cortex and insular cortex. The amygdala and insular cortex are parts of the limbic system and play a role in perception of pain and emotions due to sensory input. [4] The entorhinal cortex has been implicated in memory consolidation through its connections with the hippocampal and parahippocampal regions. [5] Finally, the orbitofrontal cortex receives sensory input from gustatory, visual and auditory pathways as well as olfactory centers and integrates this information into unified perceptions of sensory stimulus. [6]

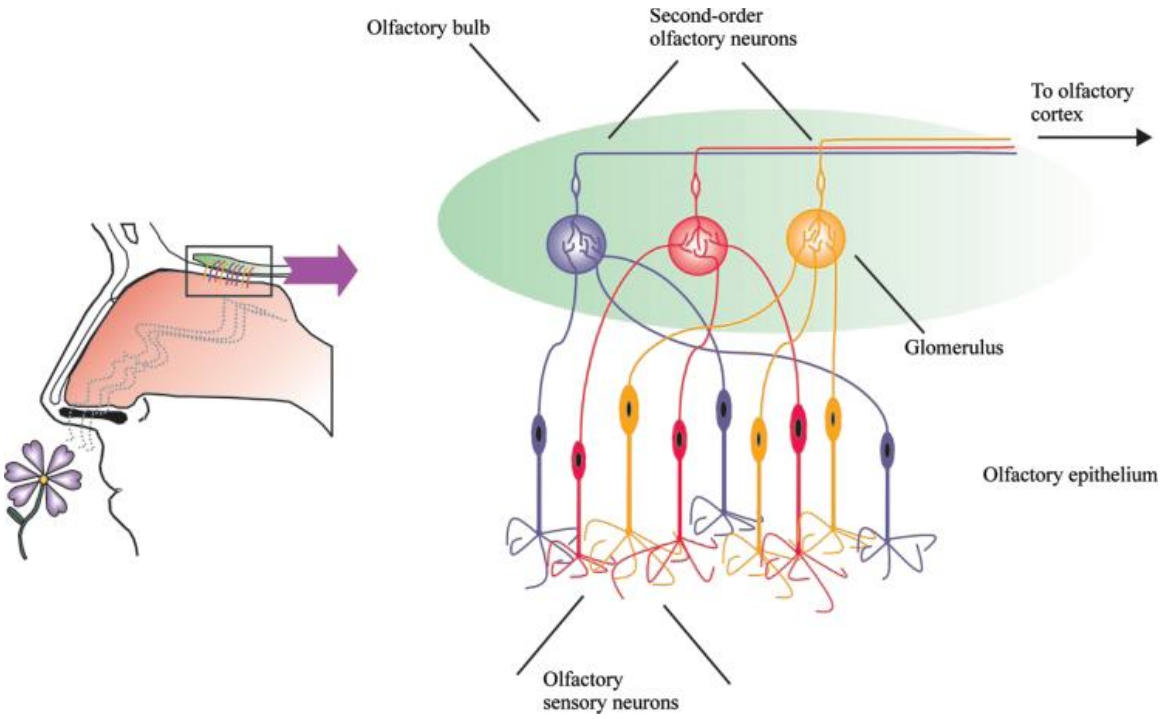

Figure 1.1: Animation of the process of olfaction from odour recognition at the olfactory epithelium to axonal trafficking to the olfactory cortex.

1.1.2. Functional Magnetic Resonance Imaging

Functional Magnetic Resonance Imaging (fMRI) is a technique that combines MRI imaging with an event-related experimental protocol to monitor changes in neural activity over a user defined time period. [7] A more detailed treatment of MRI imaging theory can be found in Appendix A. In order to distinguish between when neurons are active or in-active, the blood-oxygen level dependent (BOLD) response is used. The BOLD response arises from the difference in paramagnetic properties of oxygenated and deoxygenated haemoglobin in the blood. [8] Basically, when neurons become active the body responds by removing oxygen from the blood at an increased rate leaving more deoxygenated haemoglobin in the blood surrounding the neurons. Deoxygenated haemoglobin has more unpaired electrons (paramagnetic) creating magnetic field distortions in the blood that leads to dephasing of spins in the voxel (reduction in T2 relaxation time). The overall effect is a small decrease in signal intensity of about 8% at 1.5T. However, an increase in blood flow to the neurons after activation leads to an increase in oxygenated haemoglobin in the surrounding blood and tissue because the supply of oxygen outweighs its metabolic

extraction. This effect masks the signal decrease and the end result is an overall signal increase in the activated voxel that can be used to locate neuronal activation.

The experimental design involves repeated intervals of stimulus and no stimulus to increase statistical significance of the changes in intensity levels. Typically echo planar imaging (EPI) is used to capture fast, low resolution images to create a four dimensional image set where the time course of the intensity levels at each pixel can be correlated to the time course of the experimental protocol. [9] If the intensity change is deemed to be significant, the pixel is assigned a coloured intensity based on the level of significance as measured by a statistical score such as the t-score or F-score. These scores are used to create a map that can be overlayed on a high resolution 3D anatomical scan for localization of neural activation. The spatial resolution of fMRI is dependent on the resolution of the fMRI image set (2-5mm^3 voxel size) and the temporal resolution by the repeat time of the spin echo sequence (0.5-6s period).

1.2. Objectives

The objectives of this project are to:

1. Design an MRI compatible device capable of reliably presenting an olfactory stimulus to a subject.
2. Test the device with fMRI experiments.
3. Using experimental data, determine whether functional imaging of olfaction is feasible.

1.3. Methodology

An olfactory stimulus device was designed that allows a scent to be generated and presented to a subject whose head is positioned inside a standard MRI head coil. The device requires only a conventional hospital medical air line and a second person in the MRI suite to control the presentation and removal of the stimulus.

Functional MRI imaging for two different stimuli was performed using standard experimental protocols. Statistical analysis was performed with the assistance of open

source software (SPM 8) to search for activation patterns in the brain that correlate to the presentation of olfactory stimulus.

1.4. Scope

The scope of this project is entirely proof of concept. Functional imaging has a large role in mapping the brain function of other sensory stimuli such as touch, visual, and auditory but olfaction remains largely ignored. Validating the device design and fMRI protocol against pre-existing experimental data would help justify expansion of this research topic into a Master's or PhD level project.

2. LITERATURE REVIEW

2.1. Olfactory Stimulus Presentation

Although the presentation of olfactory stimulus has not been studied in detail in neuroscience, it has been the topic of much research in other areas such as virtual reality gaming and movies. Several unique approaches to generating and transmitting scents have been proposed to enhance the overall sensory experience. In addition to these, two MRI specific presentation devices will be reviewed for their practicality.

2.1.1. Inkjet Olfactory Display

Recently, an ink-jet cartridge based system for olfactory stimulus presentation has been proposed to assist in conducting research on the human response to odorants.[10] Working in conjunction with Canon, a group in Japan set out to minimize the amount of scent required for proper stimulation of the olfactory response. Their system boasts the ability to emit up to 12 distinct scents by taking advantage of the three printer ejection heads that can each hold four tanks. It utilizes all the same features a printer does when emitting ink onto paper with the exception that the excitation patterns dictate the types and quantity of scent being ejected. Control comes from a sensor that detects inspiration leading to the timed release of a pico-litre volume of scent into the subject's nose (Figure 2.1). The downside of this system is that it is too bulky to fit inside the MRI bore and the inkjet design is not feasible given the technology and expertise required to build a system like this.


(a)

(b)

Figure 2.1: Picture of the inkjet based olfactory stimulus injection system (a) and the system in operation (b).

2.1.2. SUBSMELL

SUBSMELL consists of a hardware component that provides olfactory stimulus and a software component for integrating smell into the movie watching experience. [11] The hardware component is a control box that reacts to software cues from the movie to release pre-loaded scents using fans to blow them out to the watchers (Figure 2.2). The fans also include blow in functionality to remove the scent. This system is simpler in its design but releasing scent into the air is not ideal given that testing will be performed in a hospital setting. Also, providing and removing stimulus in a timely, consistent manner would be difficult with this design as diffusion into the surroundings will decrease its functionality.

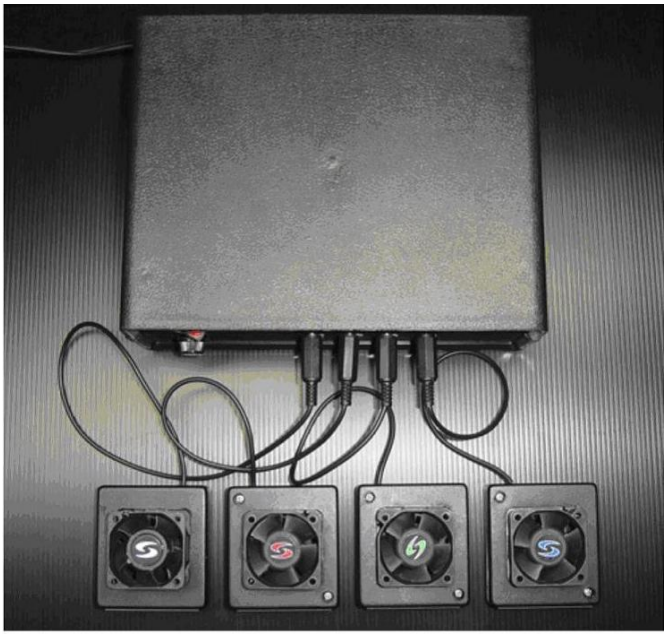

Figure 2.2: Hardware device used to deliver olfactory stimulus in the SUBSMELL system.

2.1.3. Air Cannon

The air cannon is a novel olfactory stimulus projection system that takes scented air and creates vortex rings which are then projected over a distance towards the nose of the subject.[12] Figure 2.3 demonstrates how the vortex rings are able to travel through the air by using smoke for visualization. The design consists of a rubber membrane impacted by solenoids to project air through a small aperture to create the vortex. A final prototype included a scent generator (nebulizer) and a nose tracking system for setting the direction and orientation of the cannon (Figure 2.4). Although the temporal and spatial accuracy of the air cannon are tractable, transmitting scents through the air is not ideal for this project and given that the subjects in this project are to be in close proximity to the source due to space constraints, this system is more complicated than necessary.

Figure 2.3: Demonstration of the creation of a vortex ring by means of a rubber bladder impacted by solenoids to force smoke through a small aperture.

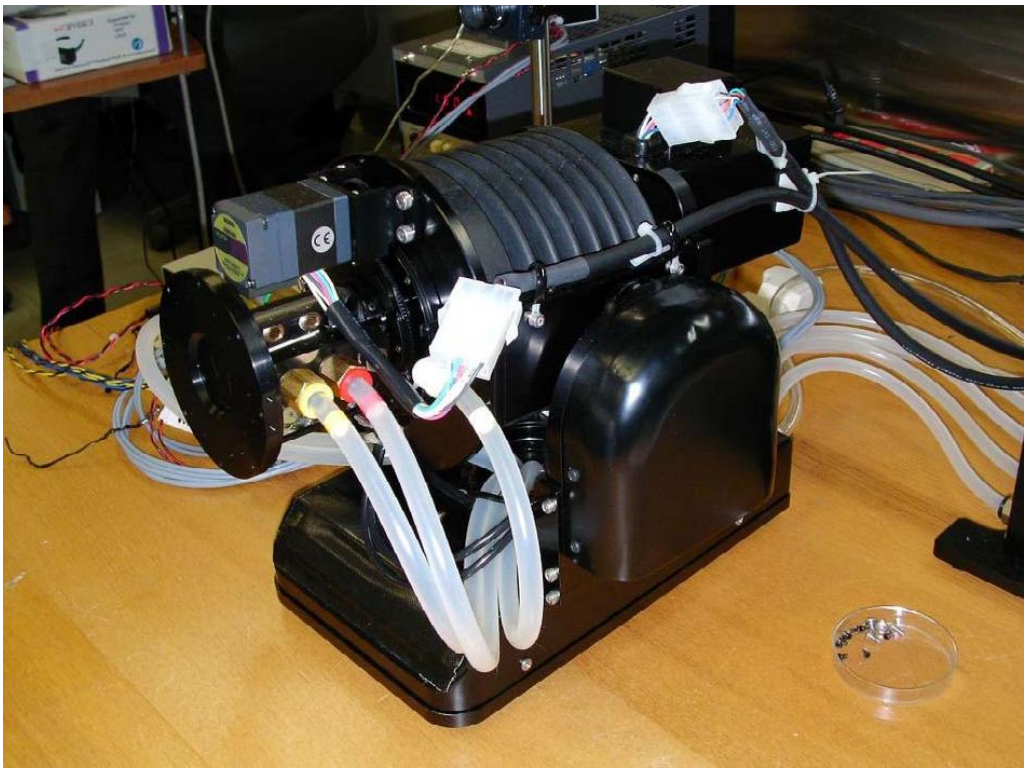

Figure 2.4: Third and final prototype of the air cannon. The final design consists of a system to eject multiple scents as well as real-time nose tracking.

2.1.4. MRI Compatible Methods

Publications do exist by groups that have attempted to deliver olfactory stimulus to subjects in an MRI suite. The techniques employed in these situations have all relied on compressed air to force stimulus through tubing to a subject wearing a ventilator mask. In one instance, an olfactometer was employed to deliver stimulus for a set of fMRI experiments. [13] This device consisted of a pressurized medical air supply and an air-dilution injection head. The air-dilution injection head was essentially a bulb compressed by an operator to force a scent into the line when respiration was sensed. Another design used a flow controller with two lines, one carrying medical air and the other a scent (Figure 2.5). [14] A manual dial was turned to open and close the line to control stimulus presentation. Both of these methods are practical for fMRI experiments and for a hospital setting which made them attractive options and the basis for the final design. Replacing manual control with an automated design was the next focus and led to research on viable actuation methods for use inside an MRI suite.

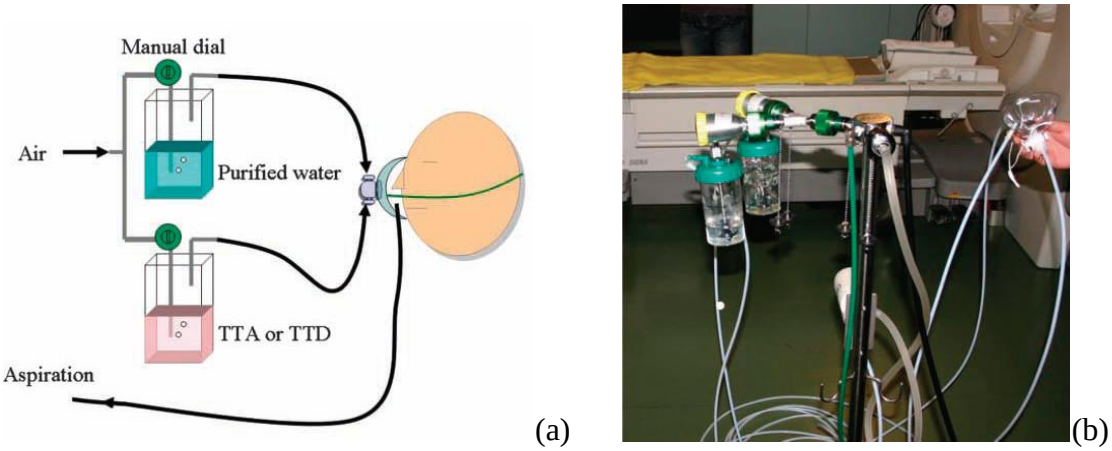

Figure 2.5: A diagram demonstrating a flow controller for delivering olfactory stimulus in fMRI experiments showing the flow of air (a) as well as the actual device used in the experiment (b).

2.2. MRI compatible control mechanisms

2.2.1. PneuStep

PneuStep is a pneumatic stepper motor that is capable of directional rotary motion in discrete increments (Figure 2.6). [15] Its motion is controlled by a remote system that sequentially pressurizes three ports on the motor. It is constructed entirely of MRI compatible parts and all control signals are encoded with fibre optics to make the system electricity free. The actuators have been implemented in a fully MRI compatible robot for prostate biopsies.[16] This motor was very promising as an actuator for the olfactory presentation device but upon contacting the designers, it was deemed to be too expensive and overcomplicated for the experimental protocol. In addition to this, the speed performance of the system degrades as the length of pneumatic hoses increases which would be problematic given the 7m distance from the hose input area in the MRI suite to the subject.

Figure 2.6: Final design of the PneuStep pneumatic stepping motor in two different sizes. All parts are MRI compatible. Note the three input nozzles for compressed air control.

2.2.2. Hydrodynamic System

A hydrodynamic actuator driven by a biologically inert, incompressible oil Orcon Hyd 32 has been developed as a possible MRI compatible system. [17] The supply oil pressure from a compressor is held at 15 to 25 bar and a directional valve controls the flow and subsequently movement of a 1 DOF actuator. It has excellent control over slow, smooth

movements and exceptional position control compared to its pneumatic counterpart but issues with fluid leaks, higher operational pressure and slower dynamics limit its usefulness for many procedures. In particular, the slow dynamics of this actuator and the potential for leaks made it an unattractive solution for control in this project.

2.3. fMRI of Smell

As mentioned above, functional imaging has not been attempted in any comprehensive manner with respect to olfaction. The experiments related to functional imaging of olfaction have focused on the emotional response to different odours and as a result the experiments are more psychology than they are neuroscience. However, these experiments do provide experimental results that can be used for the validation of the results of this project. One experiment was conducted using questionnaires to ask twenty eight participants about the strength and quality of both beta-phenyl ethyl alcohol and gamma-undecalactone as pleasant and un-pleasant odours respectively. [13] Figure 2.7 is a subset of the results where they concluded that the insula, orbitofrontal cortex, and cingulated gyrus were the regions of the brain most often activated by olfactory stimulus. A second group performed a similar series of experiments where they attempted to relate factors like sex and handedness to the emotional response to odorants. [14] Twenty eight subjects were split into four groups of seven based on handedness and gender and exposed to 90 odorants in two functional runs. The major areas of activation they found were the amygdala, cingulate gyrus and the insular cortex (Figure 2.8). Both experiments report activation in the cingulate gyrus and in areas consistent with the known anatomy of the olfactory system (amygdala, insula, orbitofrontal cortex).

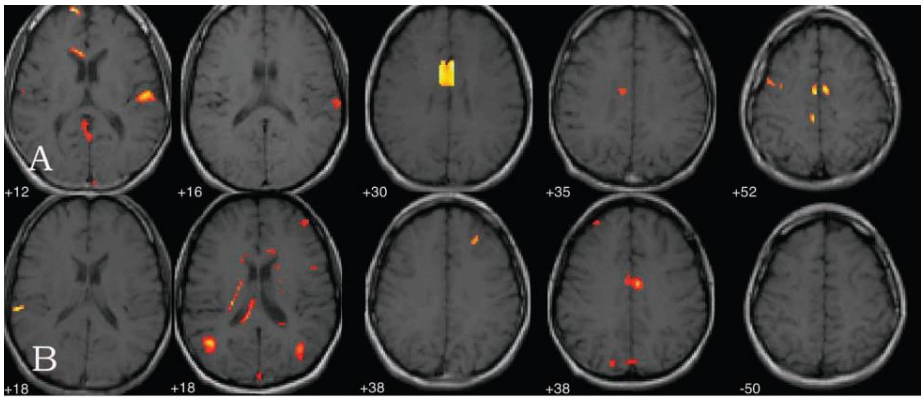

Figure 2.7: Representative fMRI slices from an experimental run where beta-phenyl ethyl alcohol (A) and gamma-undecalactone (B) were used as the olfactory stimulus. The activation in the center of the slices is attributed to the insular cortex on lower slices (+12) and the cingulated gyrus on higher slices (+30).

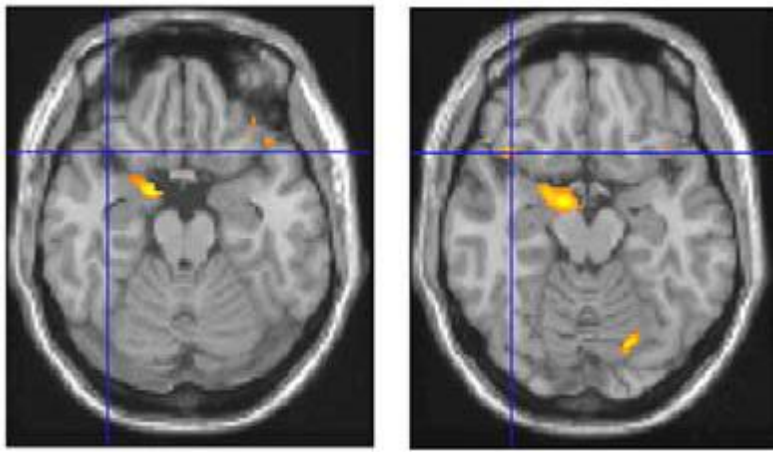

Figure 2.8: Representative fMRI results showing activation of the insula after presentation of olfactory stimulus.

3. STATEMENT OF PROBLEM / METHODOLOGY OF SOLUTION

3.1. Design Problems Encountered

The general problem was to design an MRI compatible device capable of generating and presenting olfactory stimuli for functional imaging of the neurological response to such stimuli. The design process had to take into account many limitations including the working environment, presentation control, and the nature of the olfaction. The problems associated with each are expanded on below.

3.1.1. MRI specific problems

Many problems exist when designing a device for use in an MRI setting. First, the device must be constructed of diamagnetic materials to ensure that it is not drawn into the magnet causing damage to the subject or the machine. Also, magnetism can lead to issues with data acquisition as it can disturb the homogeneity of the field reducing signal to noise. The room where the MRI is located is a Faraday cage to remove radiofrequency interference and as such there are only designated areas where electrical wiring and tubing can be passed into the room. The head coil (Figure 3.1) used to record signals from the subject restricts the design to be located either outside its physical bounds or to fit inside the small available area. Additionally, the bore diameter of the magnet (Figure 3.2) further limits the size of the device as well as increasing the length of tubing/wiring necessary to reach the subject.

Figure 3.1: Head coil used for data acquisition during the fMRI protocol.

Figure 3.2: 3T GE short bore MRI machine used for performing the fMRI experiments.

3.1.2. Device Control Problems

Designing a control system without magnetic parts is a difficult task given that most retail actuators and control valves are made of metallic materials. Consequently, almost all existing MRI compatible systems are custom made and are not commercially available. Pneumatically controlled valves and actuators made of non-metallic materials provide one solution to the problem and have been used in robotic systems for MRI-based procedures (PneuStep) but the degree of complexity and exorbitant cost associated with these products made them unrealistic for this project. Also, relying on conventional electric signals for control is not recommended given the magnetic field's ability to confound electronics during the pulsing of gradients. Therefore, encoding electric signals with fibre optics is necessary which adds another level of complexity to any control scheme as conversion systems to code electrical signals as pulses of light must be incorporated into the design.

3.1.3. Olfaction Related Problems

The process in which olfactory stimuli enter the nose and are subsequently recognized by the body is a problem unto itself. When dealing with other sensory input, it is quite easy to model the stimulus as a square pulse. For example, when performing fMRI using auditory stimulus, a typical experiment would involve turning on and off a beep at a particular frequency. This stimulus is either ON or OFF and the switch between the two states happens almost instantaneously. This makes the response easier to model as only the hemodynamic response needs to be accounted for in the analysis. With olfaction, the added complexity of stimuli having to bind their appropriate receptors as well as the nose being able to capture stimuli to make clearance difficult puts added emphasis on the quality of the presentation procedure. Quantification of olfactory stimuli is another problem partly due to the qualitative nature of olfaction and partly due to the fact that every scented liquid has a unique vapour pressure that is dependent on concentration, gas pressure and temperature. Finally, the transmission and presentation of the scent have their own problems to overcome. The scent must be created as close to the patient as possible to remove possible timing delays and the presentation procedure should allow most if not all of the scent to reach the subject's nose when required and dissipate quickly afterwards necessitating moderate to high air pressure to drive the scent.

3.2. Device Design Methodology

Initially, the design had called for the subject to control a switch that would initiate delivery of the smell and start the recording process. A pic24 microcontroller from Microchip Technologies was purchased for the purpose of relaying the control switch input to the delivery device and triggering the data acquisition hardware. The main concern had been coming up with a reliable method for controlling the delivery of the stimulus. Employing some sort of actuator that controlled the release of a concentrated scent into the air directly below the subject's nose seemed to be a good first solution. The scent was to be in a plastic tube with an end piece that could rotate to expose air holes (Figure 3.3). However, after an unsuccessful search for a compact, MRI compatible rotary actuator that was reasonably priced, the design was altered to one where a rubber flap would be controlled by positive and negative pressure to open and close over the air holes in the tube to deliver the smell (Figure 3.4). Problems also arose in this design. First, given the fact that the subject is laying down in the MRI machine, the flap could interfere with the subject's ability to breath in the scent. Second, controlling the positive and negative pressure to this tube from outside the MRI room would add a delay to the scent presentation. The problem with the presentation was overcome by employing a ventilator mask to ensure a tight seal for stimulus presentation. The timing delay could potentially be removed with a control valve inserted close to the subject. The combination of the ventilator mask and a control valve near the subject was the basis of the third proposed design (Figure 3.5). A branched air line was employed to supply the subject with medical air such that first branch would supply a continual flow of air and the second would be diverted through the smell device when the valve was opened. Thus, when the recording process was triggered, the valve would open providing a scent, and when done, it would close and the air supply would act to bleed the line. The actuator required to control the valve in close proximity to the subject proved to be very difficult to find and not economically feasible for an undergraduate project so the design was forced to move towards a manual control design where a third party initiates and removes the stimulus using predefined timing cues.

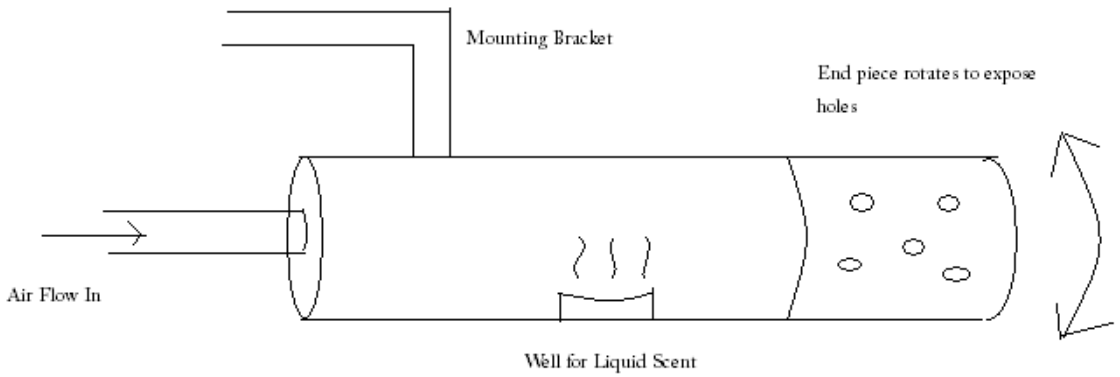

Figure 3.3: Initial control design using rotary actuation to expose holes in the plastic tube to release the enclosed scent to the subject.

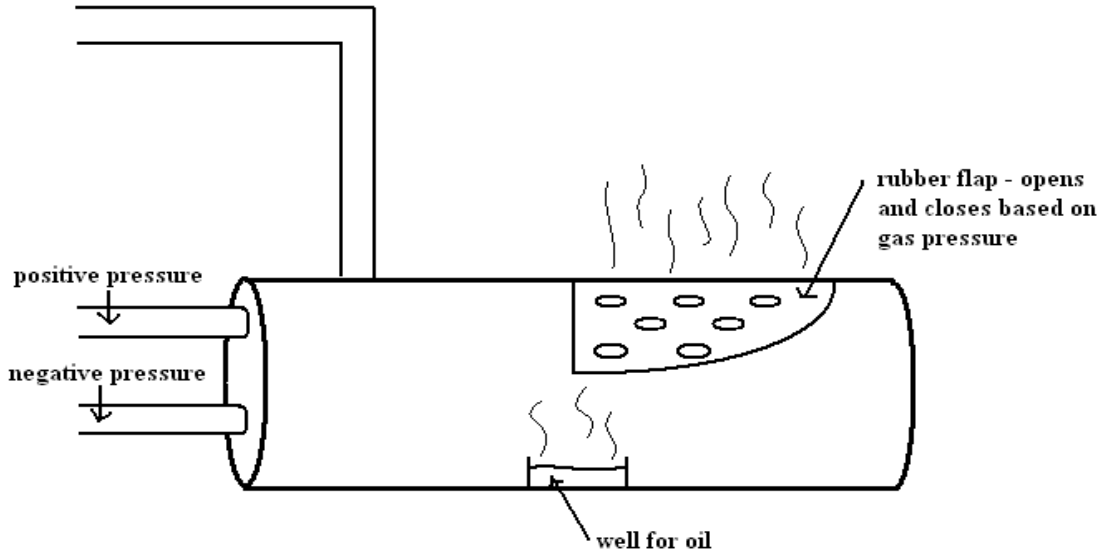

Figure 3.4: Second control design using positive and negative pressure to control a rubber flap.

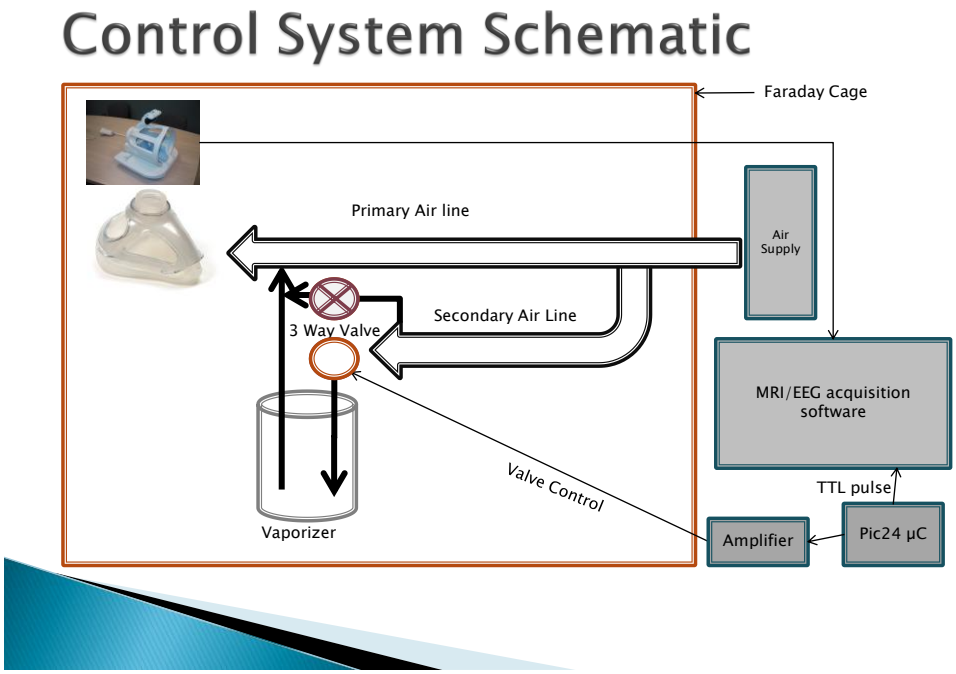

Figure 3.5: Conceptual diagram of the third design including actuated valves inside the MRI recording room.

4. DESIGN AND PROCEDURES

4.1. Final Device Design

The final design consists of a laerdol mask (mask portion of a standard ventilator mask with bulb attached) with the bag removed and sealed off with a rubber stopper (Figure 4.1). The mask contains one way valves so that inspired air comes only from the bulb and expired air exits the mask. When positioning the mask, the bulb was rotated 180 degrees to point superiorly (towards the back of the MRI bore) due the nebulizer being located back in this area. Following the flow of air, tubing is connected to the hospital medical air line and is immediately split with a Y connector so that the half the flow is directed to one side of a control valve held at the back of the MRI bore and the other half into the arm of the Erlenmeyer flask containing the aromatic fluid to be vaporized. When supplying stimulus, the pressurized flow of air causes the liquid to overcome its vapour pressure convert to its gaseous state inside the flask. In order to make sure that the air flowing into the flask did not take the least path of resistance and flow past the fluid and out of the flask, a glass tube cut to 13cm in length was inserted through a rubber #4 stopper and the end was placed less than an inch from the surface of the fluid (Figure 4.2). The scented air forced out of the flask passed into the other side of the control valve (Figure 4.3). The position of the control valve dictated whether scented air or medical air passed into the bulb of the laerdol mask for inhalation. Positioning the control valve and the nebulizer at the back of the MRI bore minimized the distance between subject and stimulus so that it could be presented and removed as quickly as possible. Sufficient air pressure from the medical air regulator (5-8 litres/min) was also required to ensure proper presentation. In order to switch between presentation and clearing states during the experimentation procedure, a second person was required to manually move the position of the control valve when prompted. Finally, all connections were sealed with Teflon tape to ensure an airtight seal throughout the device. A picture of the final device design is in Figure 4.4.

Figure 4.1: Modified ventilator mask used for olfactory stimulus presentation during the fMRI experimental trials.

Figure 4.2: Homemade nebulizer used to convert a scented liquid into a vapour for presentation to the subject during the fMRI experimental trials.

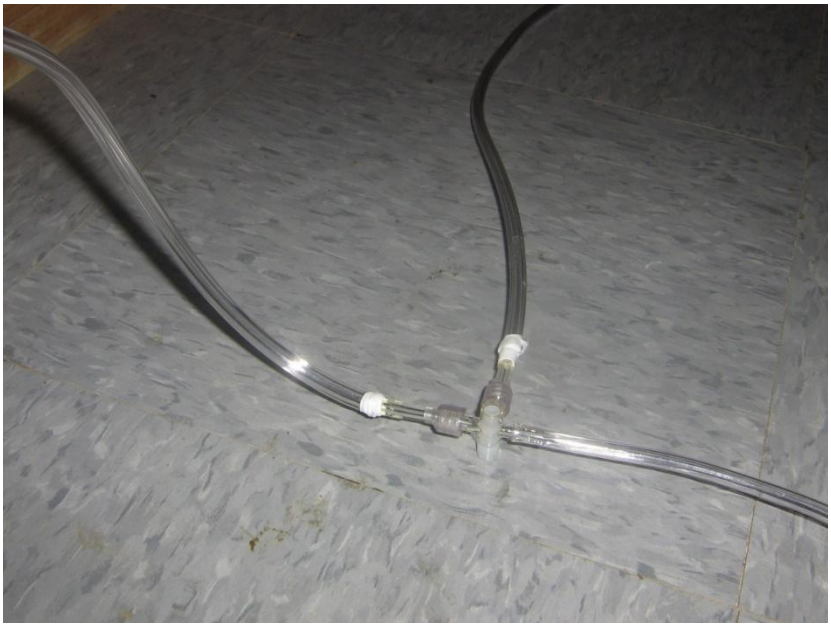

Figure 4.3: Manually operated three way control valve used to direct medical air in two directions. During stimulus presentation the air is passed through the nebulizer and during non-stimulus periods, the air flow passes directly to the subject.

Figure 4.4: Picture of the final prototype of the olfactory stimulus generation and presentation device used for fMRI experimental analysis.

4.2. Device Testing Procedure

The testing procedure consisted of three separate fMRI experimental runs. Two occurred during the same session on February 1st, 2010 and the third run occurred two weeks later on February 15th, 2010.

The first experiment used essence of orange as the stimulus in the Erlenmeyer nebulizer described above. The subject was placed on the MRI bed and their head was positioned inside the head coil. Once inside the head coil, the mask was inserted between the bars on the coil and secured to the subject's face by way of rubber straps designed for the mask (Figure 4.5). The subject was required to turn their head 30 degrees so that the mask could line up with a gap in the coil. With the mask secured to the patient, the bulb was attached and the bed was passed through to the back of the bore so that the device could be attached and the air supply turned on (Figure 4.6). Here the device was tested to ensure that the air pressure was sufficient to force the stimulus through and also to make sure the control valve was being operated correctly.

Figure 4.5: Subject after being secured inside the head coil with the ventilator mask attached.

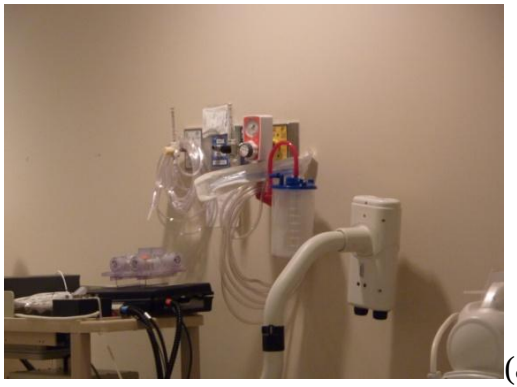
(a)

(b)

Figure 4.6: The medical air delivery system (a) and its relative position with respect to the MRI scanner (b).

The MRI scanning was performed on a 3T GE short bore scanner with a standard GE head coil. First, a calibration scan was performed to account for the extra hardware inside the scanner followed by a standard 3-D anatomical scan with 512X512 resolution and 148 slices with a slice width of 2mm. The fMRI protocol consisted of a 90 second period without stimulus followed by a 30 second period of stimulus. This was repeated 5 times for a total of 10 minutes or 600 seconds. The justification for this protocol was that 30 seconds was deemed to be an appropriate amount of time to allow for robust stimulation of the olfactory epithelium without saturating the process. Also, 90 seconds gave the device time to effectively clear the smell from the subject before the next stimulus period to maximize stimulus/ non-stimulus differences. Repeating this procedure 5 times over 10 minutes helps with statistical analysis by increasing the number of samples for the final analysis. Finally, the total length of time is short enough that the subject should be able to remain still throughout the entire experiment. The accurate timing of this protocol was achieved by facing a monitor with a clock into the MRI suite so that the control valve could be moved at the predetermined times. The scanning process for fMRI used echo planar imaging to record 23 slices with 128X128 resolution in a repetition time (TR) of 2 seconds for a total of 300 volumes (data points in the time series).

For the second experimental run performed two weeks later, the protocol remained essentially the same with two major changes. First, the stimulus was changed to a cinnamon/nutmeg blend from essence of orange for reasons that will be expanded on in

the discussion and second, the fMRI images were acquired at a more common resolution of 64X64.

4.3. Statistical Analysis of fMRI Images

For the statistical analysis of the fMRI images, the open source software SPM8 was used to provide a graphical user interface and documentation assistance for the process. This is a matlab based software developed by the Wellcome Trust Center for Neuroimaging at University College London. It has the ability to perform a variety of statistical tests on fMRI data, only those used for this project will be discussed in any detail.

The images come off the MRI scanner in dicom format and are subsequently converted to nifti-1 file format when imported into the SPM8 software. The first step in the analysis is to register the images to account for subject movement during the experimental run. This is done by choosing a representative volume to register the other image volumes to. The software uses a linear regression method with a rigid 6 parameter spatial transformation to align the slices. The first image of all volumes is aligned to the first image of the representative volume, and then all images inside each volume are aligned to the first image. A mean image is also calculated during this process for the co-registration process. Co-registration involves registering the fMRI dataset to the high resolution anatomical scan done before the fMRI experiment. Registering these two data sets ensures that when the final statistical map from the fMRI images is overlayed on the anatomical map, the correlated areas line up with their actual positions in the brain. This process is performed using the same linear regression and spatial transformation technique as in the alignment process. In this case, it is the anatomical scan that is transformed to align as closely as possible to the mean fMRI image.

Once the spatial processing on the images is complete, the next step is to specify a model. This is done by creating a square pulse approximation of the experimental protocol by defining non-stimulus periods with zeros and stimulus periods with ones. For example, when specifying the protocol for this project, a square pulse was generated with a 90 second low value followed by a 30 second high value. This was repeated 5 times for a

total of 10 minutes. The square pulse was then convolved with a hemodynamic response function (HRF) (Figure 4.7a) to model the he dynamic response to changes in neuronal activity in the blood. Convolving the two functions together gives the final model to be used for statistical analysis (Figure 4.7b).

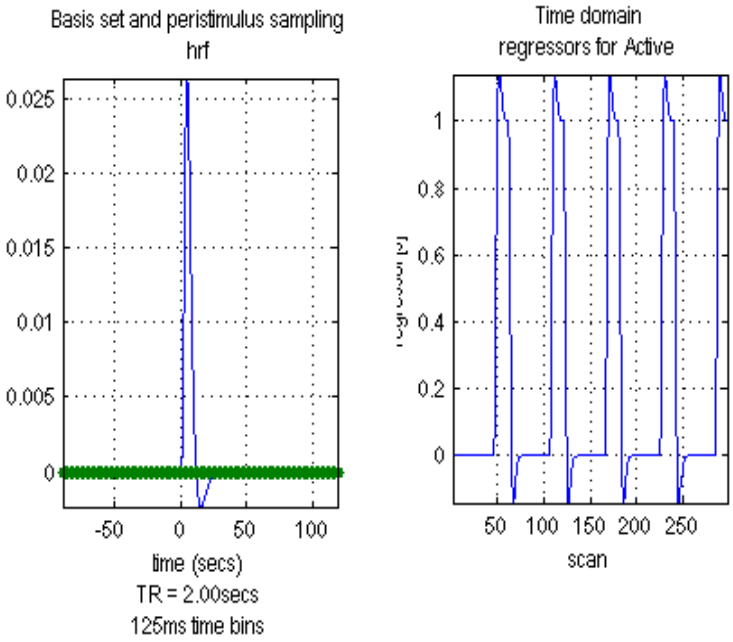

Figure 4.7: Plots showing the hemodynamic response function (HRF) as a function of magnitude vs. time (a) as well as the final model consisting of the HRF convolved with a pre-defined square wave as a function of intensity vs. scan number (b).

Next, the model parameters from the actual image data are estimated using the classical restricted maximum likelihood (ReML) method.[18,19] This process is an expansion of the general linear model to estimate parameters for the amplitude of the activation and the variance in the noise using a number of model functions. One such model function is the experimental protocol specified above while other model functions include those meant to model baseline wandering, optimize the hemodynamic response function and fit non-Gaussian noise. The theory is based on the assumption that all these functions add linearly to give the best fit model but none of the functions themselves are required to be linear. The estimated parameters for this set of functions forms the statistical parametric

map used for significance testing. T-scores or F-scores (a t-score generalized to infinite dimensionality) are calculated from the ratio of the projection of the voxel response to the model space and the remainder (error space). The larger the t-score, the easier it is to reject the null hypothesis that no activation has occurred. The t-scores are fit to the t-distribution given the N-1 degrees of freedom (N samples taken) and a p- value is assigned to assess significance of the t-scores. For this experimental protocol, activations were deemed significant with a corrected family wise error of $p<0.05$. Voxels that meet this criterion are assigned an intensity value based on their significance to create an overlay map of neuronal activation. This overlay is resized to match the resolution of the anatomical image and displayed over it to give the final image.

5. RESULTS AND DISCUSSION

The first trial consisted of two fMRI experimental runs. The first run was not used for analysis as some issues arose with the pressure of the medical air used to transmit the stimulus through the tubing as well as control of the valve. As a result the pre-planned experimental protocol was not followed well enough to use this run for analysis.

The issues were addressed for the second run and the protocol was followed as described previously. Images were attained from statistical analysis but due to the 3-D nature of the overlay, only representative slices displaying areas of activation will be discussed below.

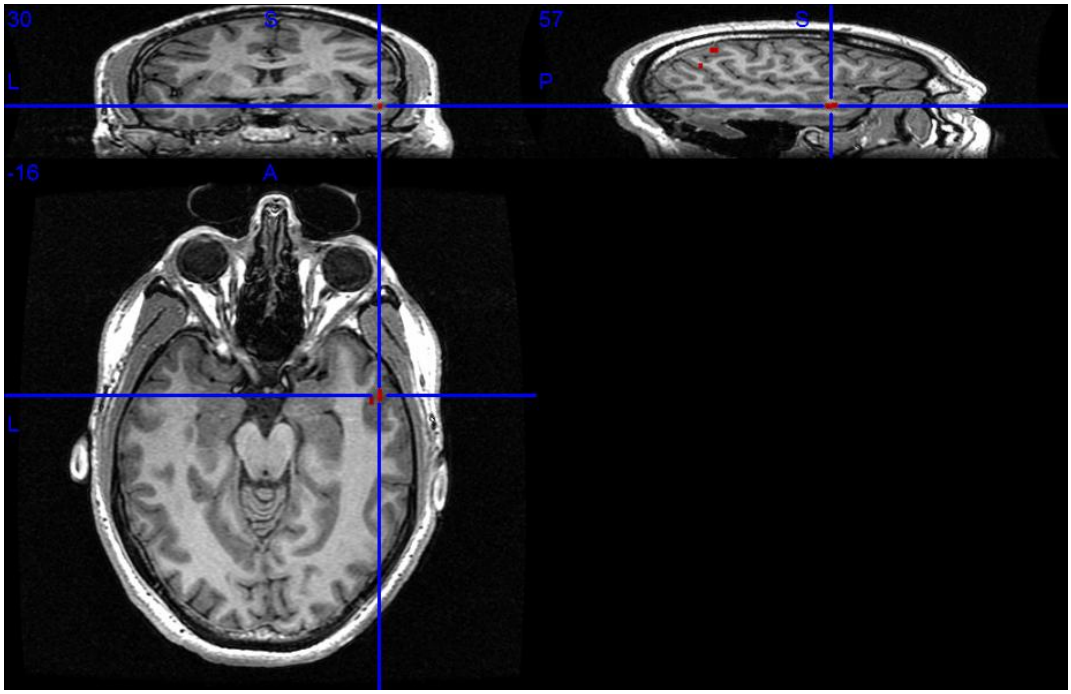

Figure 5.1: fMRI images from the second experimental run with the crosshairs pointing towards apparent activation in the temporal lobe of the subject. The top left view is a coronal view, top right a sagittal view and bottom left is the axial view.

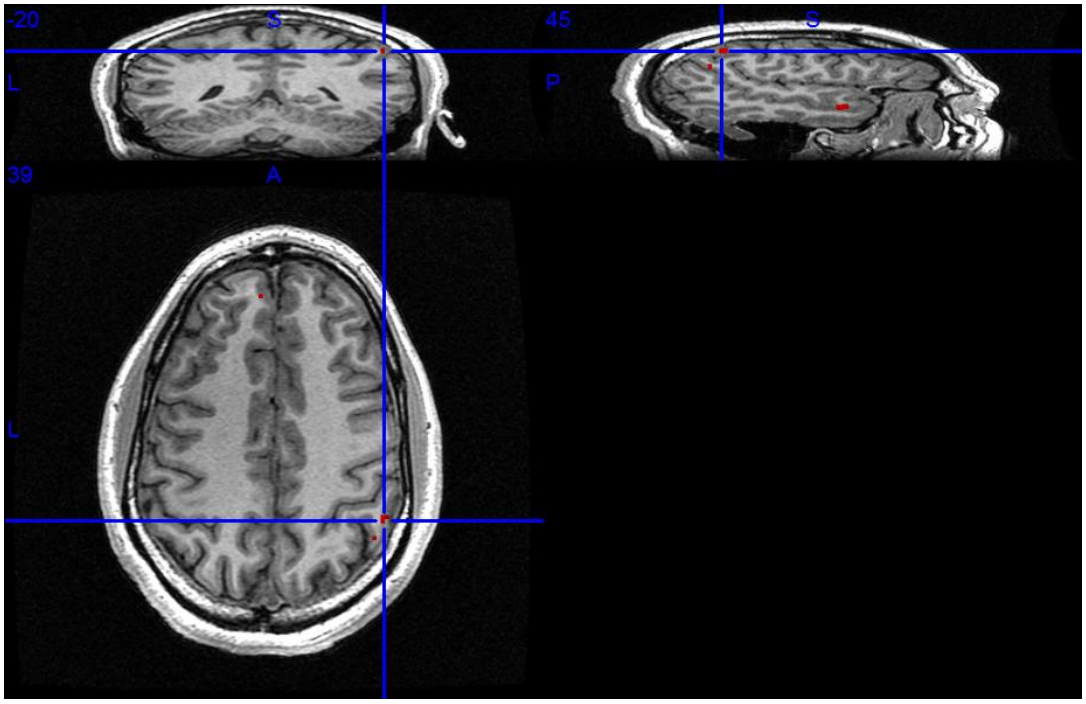

Figure 5.2: fMRI images from the second experimental run with the crosshairs pointing towards apparent activation in the parietal lobe of the subject. The top left view is a coronal view, top right a sagittal view and bottom left is the axial view.

Figure 5.1 and 5.2 are representative images of activated areas from the second experimental run of trial 1. Activation is seen in the temporal lobe (Figure 5.1) as well as the parietal lobe (Figure 5.2). These areas don't necessarily fit with those expected to be activated by olfactory stimulus given the currently accepted model of olfaction. These results could have arisen for a couple of reasons; the first concerns the stimulus used. The stimulus in trial one was essence of orange which had a very sweet citrusy smell. This smell was pleasant and easily recognizable which initially made it a great candidate for these experiments. However, the laerdol mask used for presenting the stimulus was made of plastic and new plastics have a sweet smell of their own. The result is that the essence of orange was not as distinguishable from the background plastic smell as might be necessary to get robust activation. The second is that during the first trial of experiments, by the time the second fMRI experiment was performed, the subject had been in the MRI breathing dry medical air for approximately half an hour. The result was that they experienced drying of the olfactory epithelium which they attempted to

compensate for by breathing deeply during the stimulus periods. This could have led to correlated activity related to the change in respiratory activity or due to flaring of the nostrils that occurred. Overall this experimental run served as a means to improve the protocol by revisiting the stimulus to be given and to educate the subject as to the importance of controlling respiration and movement during the procedure. The second trial took these issues into consideration resulting in the images seen in Figure 5.3, 5.4 and 5.5.

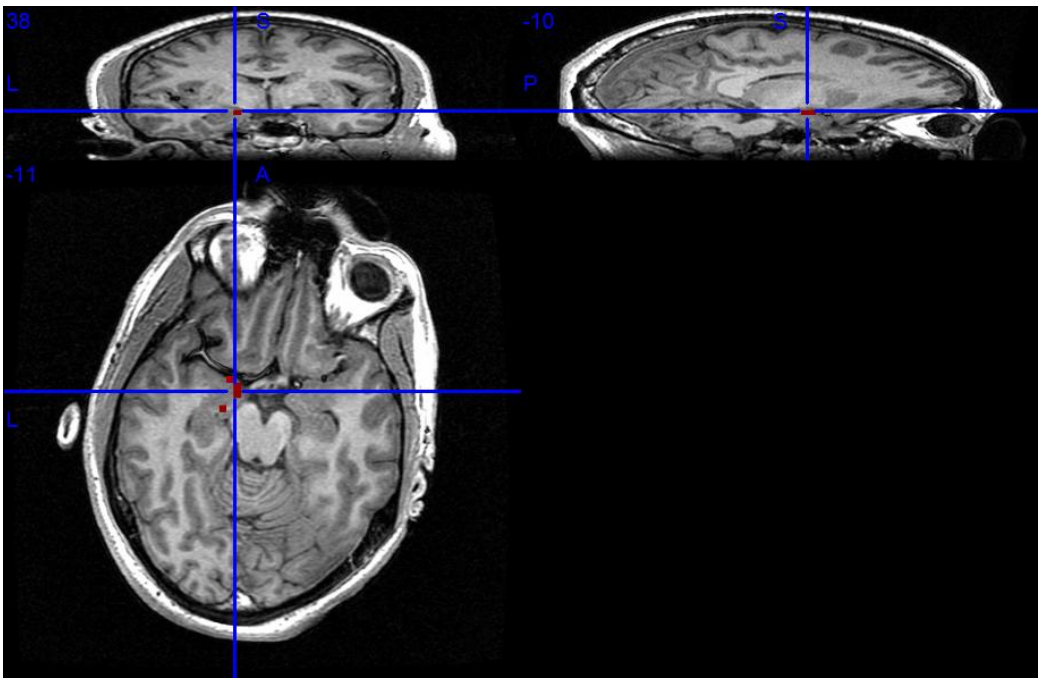

Figure 5.3: fMRI images from the third experimental run with the crosshairs pointing towards apparent activation in the insular cortex and limbic related centers. The top left view is a coronal view, top right a sagittal view and bottom left is the axial view.

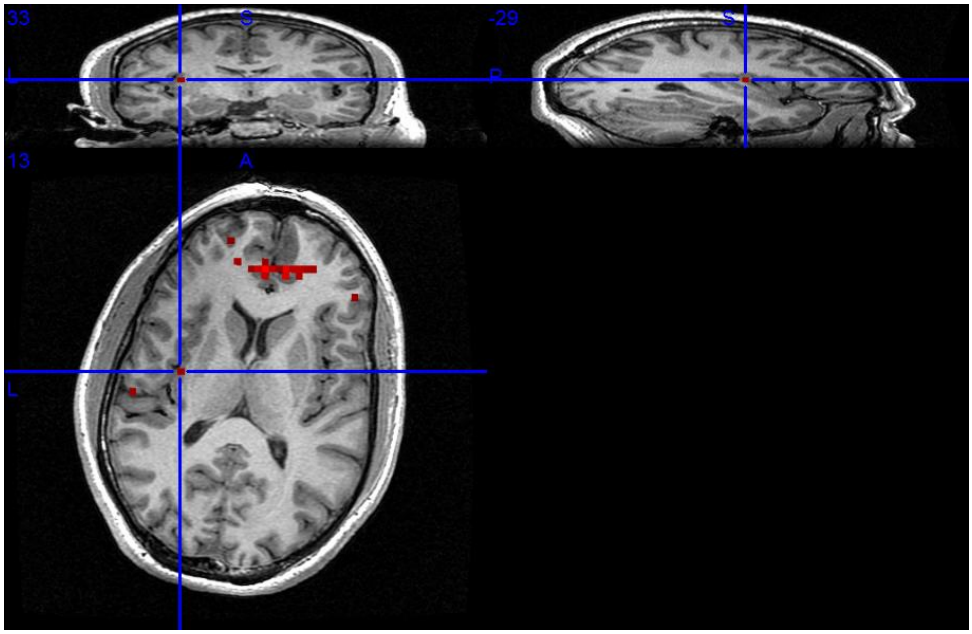

Figure 5.4: fMRI images from the third experimental run with the crosshairs pointing towards apparent activation in the amygdala of the subject. The top left view is a coronal view, top right a sagittal view and bottom left is the axial view.

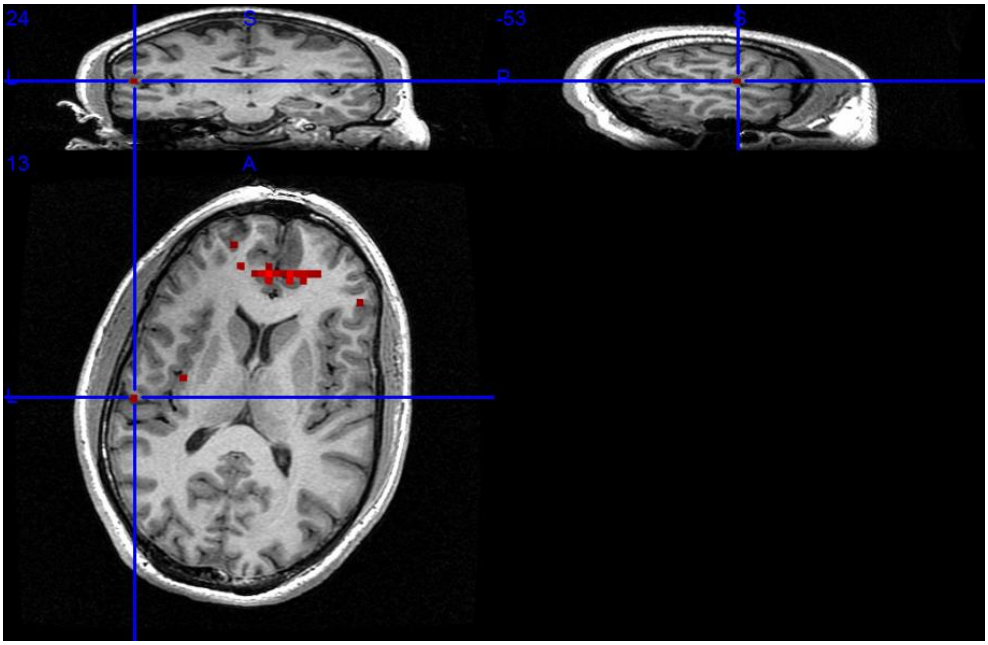

Figure 5.5: fMRI images from the third experimental run with the crosshairs pointing towards apparent activation in the temporal lobe of the subject. The top left view is a coronal view, top right a sagittal view and bottom left is the axial view.

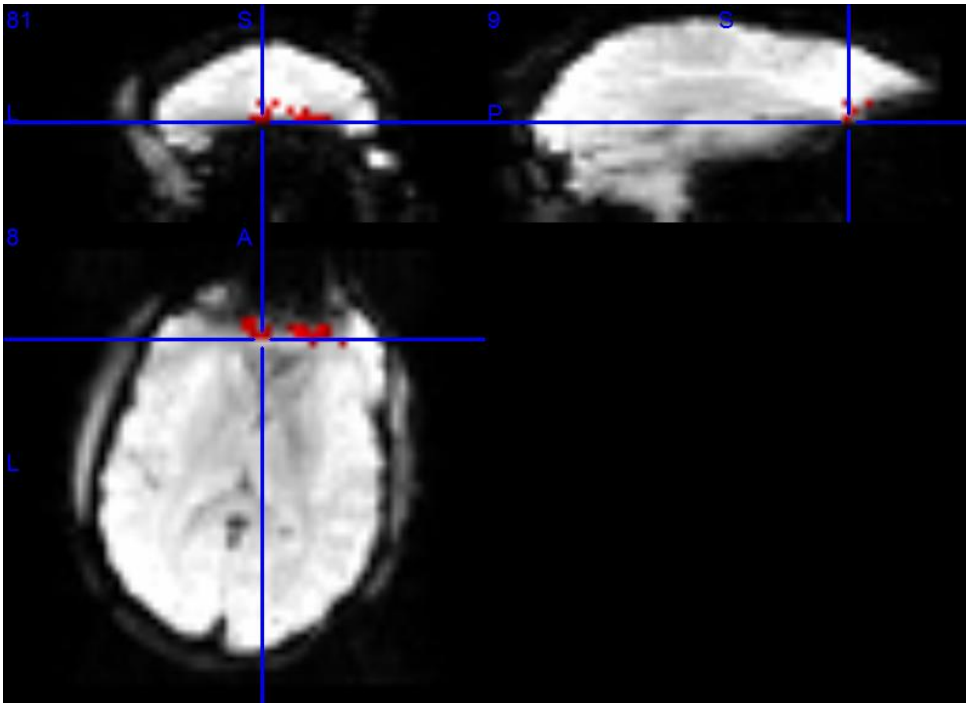

Figure 5.6: An image showing the activation map overlayed on the fMRI image set to demonstrate that the apparent high activation in the frontal cortex is likely due to a susceptibility artefact due to the sharp change in magnetic susceptibility at the tissue-air interface.

As evident from Figure 5.3, this trial run shows evidence of strongly correlated activation in the deeper areas more normally associated with olfactory stimulus. This includes areas of the limbic system such as the amygdala (Figure 5.4) and the insula (Figure 5.3). Correlated activation in these areas has been demonstrated in other papers on this topic. [15, 16] Activation in the temporal lobe (Figure 5.5) is still evident similar to what was seen in the first trial run. Correlation in this area is likely not due to olfaction but may be associated with the chance correlation of auditory inputs from the noise of the MRI gradients during the acquisition process. There also appears to be a large amount of activity in the frontal cortex and initially this appeared promising given the known association of olfaction with the orbitofrontal cortex. However, when overlaying the image on an fMRI volume (Figure 5.6), the activation lies on the boundary of the image making it likely that this activation is due to noise from susceptibility artefacts around the sinuses so it has been ignored.

6. CONCLUSIONS AND RECOMMENDATIONS

The device design, while simplistic, worked well for the functional imaging experiments it was required for. Once a proper stimulus was chosen and the air pressure was increased to a useable level, the device worked flawlessly. It was able to provide stimulus consistently and in a timely manner given proper operational control by the person turning the control valve. If the experiments were done in a timely fashion, the issues associated with drying of the olfactory epithelium could be avoided. Finally, experience being scanned by an MRI helped with controlling the subjects breathing rate and extraneous movements as nerves were less likely to be an issue.

A goal of the project was to demonstrate whether functional imaging of the olfactory response is feasible given a properly designed stimulus device. The results of the experiments that were performed are promising with that goal in mind. The last trial in particular, in which many of the errors of the previous two trials had been corrected, demonstrates that with an appropriate stimulus and an accurately performed experimental protocol, the functional activation of at least some of the olfactory centers of the brain can be visualized. Even more promising, these areas correlate well with previous studies done on olfaction reviewed in section 2.3.

With promising preliminary results such as these, attempting this as a Master's or PhD thesis project is justifiable and would allow a more robust treatment of the device design and experimental protocol to be undertaken including an expansion of some features of the project such as:

1) **Automation of the device**

   Means of automating devices in MRI environments do exist and include pneumatic and hydraulic systems as mentioned previously. This would remove human error from control of the system as well as automating timing sequences.

2) **Quantification of stimuli**

The ability to quantify the amount of stimulus delivered to the subject would add a degree of complexity to the problem that could have interesting results. This idea was considered in the design process as it would be similar to quantified delivery of gaseous anaesthetic. Quantification in this context requires an MRI compatible vaporizer that uses the vapour pressure of the liquid and the gas pressure driving the vapour to quantify the amount of gas emitted. Vaporizers of this nature can be found as parts of commercially available MRI compatible anaesthetic systems.

3) **Expansion of the types of stimuli.**

Many different classes of stimuli could be used to elicit different responses. Pleasant vs. Unpleasant has been the largest area of research for olfaction but many other areas could be examined. For example, pheromones are a group of naturally occurring odorants that could be examined in more detail to determine what kind of neurological response occurs when exposed. Drug abuse could be another focus as users of drugs like marijuana and crack cocaine could be imaged as they inhale their respective drugs for any neurological activity that could be attributed to underlying addiction.

4) **Optimizing the protocol by changing stimulus periods.**

The experimental protocol chosen for this project was conservative with regards to the amount of time for robust activation as well as the length of time required to effectively clear the stimulus. Other common protocols have called for a symmetrical 30s ON and 30s OFF model [15] as well as 60s ON and 60s OFF [16]. With consistent access to a research MRI, optimization of the experimental protocol could be undertaken so that maximal activation is viewed in the functional images. This would include increasing and decreasing stimulus times, increasing and decreasing time allotted for clearance of the stimulus as well as increasing the number of stimulus cycles to increase statistical significance.

A. APPENDICES

A.1 Magnetic Resonance Imaging

Magnetic resonance imaging (MRI) is an extension of nuclear magnetic resonance (NMR) in which the spectral readout of the proton (^{1}H) content of tissue is localized using magnetic field gradients in the X, Y and Z directions.

The magnetic resonance phenomenon arises due to the absorption and emission of energy supplied to protons by timed radiofrequency pulses. When a large external magnetic field is applied in the Z direction, protons precess around that field at a frequency determined by the magnitude of the magnetic field and the gyromagnetic ratio of the nucleus given by the equation:

$$\omega_o = \gamma \beta_o \text{ radians/s.}$$

γ= gyromagnetic ratio of the nucleus and β_o= applied external magnetic field.

An applied radiofrequency pulse will provide energy to the precessing nuclei that cause them to be knocked over to the transverse XY plane. When the pulse is removed, the nuclei gradually relax back to their original orientation in the Z plane emitting the energy initially absorbed (Figure A.1). This relaxation gives rise to two constants inherent to the nucleus being imaged. These are the T1 relaxation time, which is the time constant for the exponential growth of the magnetization on the longitudinal (Z) axis and the T2 relaxation time, which is the time constant for an exponential decrease of the magnetization in the transverse plane. Radiofrequency coils perpendicular to the transverse plane detect this relaxation energy as an induced current and the time varying value of this current is recorded as a free induction decay (FID) waveform. (Figure A.2) These signals are recorded and processed for multiple cycles of varying gradients to fill a frequency space referred to as k-space. Once filled, an inverse Fourier transform can be used to generate the image (Figure A.3).

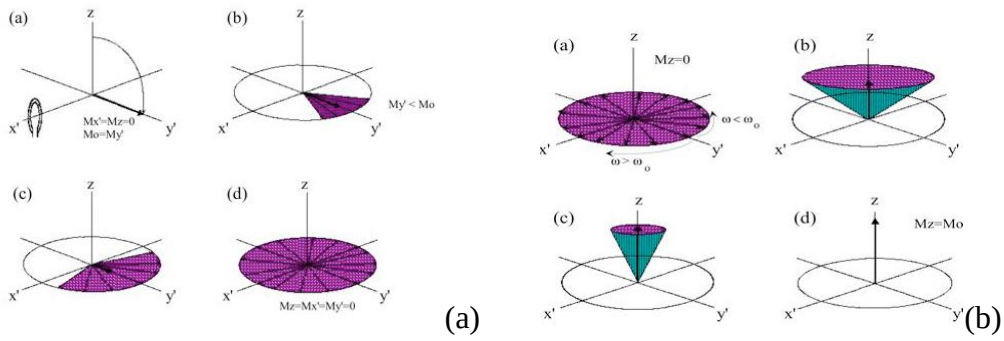

Figure A.1: Animations demonstrating the fundamental principles of MRI. Application of a RF pulse causes the proton spin to be flipped to the transverse plane (a.a) and removal causes the spins to lose energy and diphase in both the transverse and longitudinal plane (a.b-d,b.a-d). (Noseworthy, 2010)

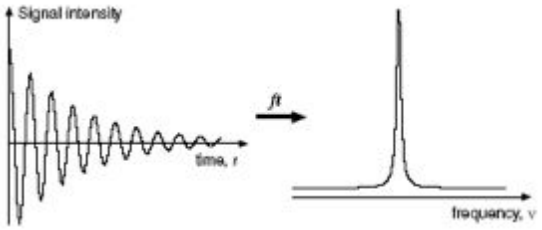

Figure A.2: Example of a free induction decay waveform recorded from a radiofrequency coil during magnetic resonance imaging data acquisition. (Noseworthy, 2010)

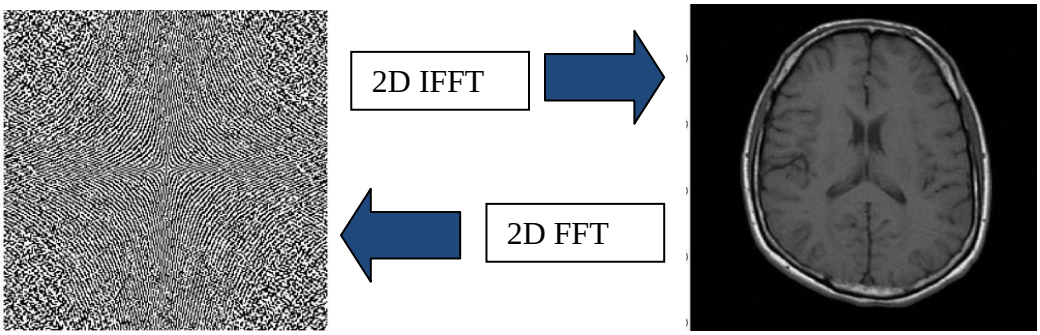

Figure A.3: Fourier relationship between k-space and image space. (Noseworthy, 2010)

REFERENCES

1. Glusman G, Yanai I, Rubin I, Lancet D. The complete human olfactory subgenome. *Genome Res* 11(5): 685-702, 2001.
2. Buck L and Axel R. A novel multigene family may encode odorant receptors: a molecular basis for odour recognition. Cell 65: 175-187, 1991.
3. Mombaerts P. Seven-transmembrane proteins as odorant and chemosensory receptors. Science 286: 707-711, 1999.
4. Hudry J, Ryvlin P, Royet JP, Mauguiere F. Odorants elicit evoked potentials in the human amygdala. Cereb Cortex 11(7): 619-27, 2001.
5. Dade LA, Zatorre RJ, Jones-Gotman M. Olfactory learning: convergent findings from lesion and brain imaging studies in humans. Brain 125(Pt 1): 86-101, 2002.
6. Yamamoto T, Oomura Y, Nishino H, Aou S, Nakano Y, Nemoto S. Monkey orbitofrontal neuron activity during emotional and feeding behaviours. Brain Res Bull 12(4): 441-3, 1984.
7. Buxton, RB. *Introduction to Functional Magnetic Resonance Imaging*. Cambridge University Press, 2002.
8. Ogawa S, Lee T-M, Nayak, AS, Glynn P. Oxygenation-sensitive contrast in magnetic resonance image of rodent brain at high magnetic fields. Magn. Res. Med. 14: 68-78, 1990.
9. Schmitt F, Stehling MK, Turner R. *Echo Planar Imaging: Theory, Technique and Applications*. Springer: Berlin, 1998.
10. Sato J, Ohtsu K, Bannai K, Okada K.Effective Presentation Technique of Scent Using Small Quantities of Odour Ejection. *IEEE Virtual Reality* 3: 151-158, 2009.
11. Pornpanomchai C, Threekhunprapa A, Pongrasamiroj K, Sukklay P. SUBSMELL: Multimedia with a Simple Olfactory Display. LNCS 5414: 462–472, 2009.
12. Yanagida Y, Kawato S, Noma H, Tomono A,Tetsutani, N. Projection-Based Olfactory Display with Nose Tracking. IEEE Virtual Reality 3: 43-50, 2004.

13. Katata K, Sakai N, Doi K, Kawamitsu H, Fujii M, Sugimura K, Nibu, K-I. Functional MRI of regional brain responses to ‘pleasant’ and ‘unpleasant’ odours. Acta Oto-Laryngologica 129: 85-90, 2009.
14. Royet JP, Plailly J, Delon-Martin C, Kareken DA, Segebarth C. fMRI of emotional responses to odours: influence of hedonic valence and judgment, handedness, and gender. Neuroimage 20(2):713-28, 2003.
15. Stoianovici D, Patriciu A,Petrisor D, Mazilu D,Kavoussi L. A New Type of Motor: Pneumatic Step Motor. *IEEE/ASME Transactions On Mechatronics* 12:98-106, 2007.
16. Song D, Petrisor D, Muntener M, Mozer P, Vigaru B, Patriciu A, Schar M, Stoianovici D. MRI-compatible pneumatic robot (MRBot) for prostate brachytherapy: Preclinical evaluation of feasibility and accuracy. Brachytherapy Volume 7(2):177-178, 2008.
17. Yu N, Hollnagel C, Blickenstorfer A, Kollias SS, Riener R. Comparison of MRI compatible systems with hydrodynamic and pneumatic actuation. IEEE/ASMET Transactions on Mechatronics 13(3): 268-277, 2008.
18. Friston KG, Glaser DE, Henson RNA, Kiebel S, Phillips C, and Ashburner J. Classical and Bayesian Inference in Neuroimaging: Applications. NeuroImage 16, 484–512, 2002.
19. Friston KG, Glaser DE, Henson RNA, Kiebel S, Phillips C, and Ashburner J. Classical and Bayesian Inference in Neuroimaging: Theory. NeuroImage 16, 465–483, 2002.

VITAE

Shawn Keating, born April 30, 1980, was raised in Saskatchewan where he received his early primary and secondary education. His postsecondary education includes a Bachelor of Science degree in Cellular, Molecular and Microbial Biology from the University of Calgary in 2006 as well as a soon to be conferred Bachelor of Engineering degree in Electrical and Biomedical Engineering from McMaster University. In September 2010 he will begin his pursuit of a Master's degree in Medical Biophysics at the University of Toronto.

Shawn's awards and honours include an NSERC USRA grant for the summer of 2009, the senate scholarship for exemplary grades for the 2008/09 school year, and Dean's Honour List for each of his four years at McMaster University.

His extracurricular interests include being active in his student society, Bioengineering at McMaster Society, where he served as VP Internal for the 2008/09 school year and as President for the 2009/10 year.